From:	GROOM Jeremy
To:	Henning, Alan; Leinenbach, Peter; MICHIE Ryan; Lightcap, Scott
Subject:	RipStream downstream submitted manuscript
Date:	Wednesday, June 25, 2014 4:10:22 PM
Attachments:	Davis et al. submitted_WRR.pdf

Hi all,

I've attached the submitted draft manuscript of *Newton's law of cooling for modeling downstream temperature response to timber harvest. L.J. Davis, M. Reiter, J.D. Groom.* I submitted it last week, and presented a figure from the manuscript at the Board workshop on Monday. I'm excited about the manuscript and hope it proves useful. I am providing the manuscript at submitted. Two caveats and one note:

Note: the figures appear in a variety of sizes. This will no doubt get remedied as we move forward.

Caveats: This manuscript is still in process. It will no doubt change as it undergoes review; therefore, it needs to be considered as a draft document. Previous versions of the document should be disregarded, as changes have been purposefully made between earlier versions and this one.

Hopefully it'll make it through the various publication hurdles, and do so quickly! Thanks for your interest,

Jeremy

Jeremy Groom
Monitoring Coordinator
Private Forests Division
Oregon Department of Forestry
2600 State St.
Salem, OR 97310-0340
503-945-7394

Newton's Law of Cooling for Modeling Downstream Temperature Response to Timber Harvest

Lawrence J. Davis,[1] Maryanne Reiter,[2] Jeremiah D. Groom,[3]

[1]D3 Scientific, Springfield, Oregon, USA.

[2]Weyerhaueser, NR Springfield, Oregon, USA.

[3]Oregon Department of Forestry, Salem, OR, USA.

Abstract. We have applied a Newton's Law of cooling model to examine the downstream water temperature response of small and medium-sized streams to timber harvest activity in riparian environments throughout the Oregon Coast Range. The model requires measured stream gradient, width, depth and upstream control reach temperatures as inputs and contains two free parameters which were determined by fitting the model to measured stream temperature data. This method reproduces the measured downstream temperature responses to within $0.4C^{\circ}$ for 15 of the 16 streams studied and provides insight into the physical sources of site-to-site variation among those responses. We also use the model to examine how the magnitude of downstream temperature changes depend on distance from the harvest reach. We estimate that the temperature change 300m downstream of the harvest reach can range from 83% to less than 1% of the temperature change which occurred within the harvest reach, depending primarily on the downstream width, depth, and gradient.

1. Introduction

Stream temperature response to timber harvest has been widely studied for decades in the Pacific Northwest (*Brazier and Brown* [1973]; *Caldwell et al.* [1991]; *Zwieniecki and Newton* [1999]; *Gomi et al.* [2006]; *Gravelle and Link* [2007]; *Groom et. al.* [2011a]; *Groom et. al.* [2011b]; *Janisch et al.* [2011]; *Rex et al.* [2012]; *Cole and Newton* [2013]; *Kibler et. al.* [2013]). The majority of studies examined the local, short-term temperature response to harvest while a few have examined changes in temperature downstream of a harvest unit (e.g., *Caldwell et al.* [1991]; *Zwieniecki and Newton* [1999]). In their review of timber harvest effects on stream temperature, *Moore et. al.* [2005] found that only three of the numerous studies they reviewed attempted to quantify the processes governing changes in stream temperature as a stream flows into a more densely shaded downstream reach (*Brown et. al.* [1971]; *Story et. al.* [2003]; *Johnson* [2004]). They go on further to say "Clearly, more research is required to clarify the mechanisms responsible for downstream cooling and how they respond to local conditions." The goal of this study is to advance understanding of stream temperature dynamics below individual timber harvest units within the Oregon Coast Range and quantitatively analyze and predict the downstream response of the maximum stream temperature to harvest activity.

Models for predicting stream temperature response from reach to basin scales generally fall into two basic categories: statistical or physical, each with advantages and disadvantages, depending on objectives. The statistical models (e.g. stochastic and regression: *Donato* [2002]; *Neumann et. al.* [2003]) can be very powerful in identifying the dominant factors driving changes to stream temperature, and applied appropriately, may allow for prediction of these changes. However, statistical models do not directly illuminate the underlying physical mechanisms that give rise to the parameter relationships they identify. On the other hand physical models are used to study the specific mechanisms driving stream temperature dynamics. The majority of physical models employ a heat budget approach to identify the net rate of thermal energy transfer into the stream from which the rate of temperature change can be calculated if the heat capacity of the stream is known (*Caissie* [2006]; *Brown* [1969]; *Edinger et al.* [1968]; *Bogan et al.* [2003]). Such heat budget models are useful tools for investigating which stream properties are most important in determining stream temperature, and can provide insight into the physics governing stream temperature dynamics. As with any model, the accuracy of heat budget models depends on the accuracy of the input variables, which must be measured. The number of input variables required to run these models can be quite large; they are often difficult, expensive, and time consuming to accurately measure, and they can vary significantly on the reach scale (*Sugimoto et al.* [1997]; *Sinkrot et al.* [1993]; *Dent et al.* [2008]; *Johnson* [2003] and *Caissie* [2006]). Consequently, non-local values for variables such as wind speed, cloud cover, etc. are often used and the uncertainties introduced by such substitution can sometimes effectively negate the advantages provided by the models. In order to address some of these difficulties we have employed a Newton's Law of Cooling model to analyze and predict downstream maximum temperature responses to timber harvest observed as part of a larger study of forested streams in the Oregon Coast Range.

The before-after control-impact (BACI) study called Riparian Function and Stream Temperature (referred to as RipStream) was initiated in 2002 to examine the effects of forest harvest with buffers on stream temperature and riparian function in first through third order streams in the Oregon Coast Range. Several publications have resulted from the study which have established background variability (*Dent et al.* [2008]), effects of harvest in relation to state water quality standards for stream temperature (*Groom et. al.* [2011b]), and change in treatment reach temperature due to harvest with explanatory variables (*Groom et. al.* [2011a]). We have used a Newton's Law of Cooling (NLC) model to analyze the downstream response because NLC models require relatively few measured stream variables as inputs and can thus be especially powerful when limited stream data are available (*Caissie et. al.* [2005]). The specific NLC model we used required only stream channel width (wetted), maximum channel depth, stream gradient, and the change in upstream control reach maximum temperature in order to reproduce observed downstream maximum temperature responses. We have successfully applied the model to analyze and understand changes in maximum stream temperature occurring within downstream reaches up to $\approx 300m$ below individual harvest units. The model together with the results of this new analysis provide managers, regulators, and landowners with additional information regarding the processes and factors governing temperature behavior downstream of harvest units. In the following sections we discuss the field study used to test the NLC model, the details of the model itself, the conditions under which it is valid, and the potential of the model for use in stream temperature data analysis and prediction.

2. Field Methods

The pertinent study information is described here; however, for a full description of data collection and field protocols see *Groom et. al.* [2011b]. Also see *Dent et al.* [2008] for a map of the study area and full description of site selection criteria and *Groom et.*

al. [2011a] for a summary of site characteristics including channel and riparian vegetation statistics pre-and-post-harvest.

Criteria for stream selection included no beaver influence (dams or disturbed vegetation), average annual flow rates of 283 L/s or less, and treatment reaches harvested according to state and private forest prescriptions for fish-bearing streams. Forest land owners volunteered 33 sites that met the selection criteria. For all 33 sites temperature was monitored on at least two reaches: an upstream control reach and a treatment reach (harvest with buffers). An additional downstream reach temperature was monitored at a subset of sites. Study parameters required the downstream reach to be relatively homogeneous with intact riparian vegetation and no major tributaries in order to minimize confounding variables. These criteria resulted in only 18 of the 33 study sites receiving a downstream temperature probe. The downstream probes were located 180m to 345m below the lower harvest unit boundary as seen in Figure 1. At each probe location stream temperature was monitored for two years before timber harvest and five years after harvest. Temperature probes were deployed at each site between June and September. Temperature probes recorded stream temperature on an hourly basis with a stated accuracy of $0.2C^{\circ}$ and a precision of $0.01C^{\circ}$ (Optic Stowaway Temp and HOBO Water Temp Pro data loggers, Onset Computer Corporation, Bourne, Massachusetts). Pre-and post-deployment quality control checks determined thermistor accuracies. Temperature was monitored at the upstream edge of the control reaches (probe 1W), at the upstream and downstream boundaries of the treatment (harvested) reach (probes 2W and 3W), and 180m to 345m downstream of treatment reaches (probe 4W), as depicted in Figure 1. Data from the summer immediately before and immediately after harvest were used.

If data from one of the immediate pre or post-harvest years was not available then data from the next adjacent year were used for this analysis (e.g., 2 years pre-harvest or 2-years post-harvest). Sites with two consecutive years of unavailable data were not used. As a result of these temporal data constraints, 16 of the 18 downstream sites were used in this analysis. Other data collected for the study include: maximum stream depth, bank full, and wetted width, shade and stream gradient. These parameters were measured within each reach at 60 m intervals. Channel metrics were collected according to *Kaufman and Robison* [1998]. Shade was measured using hemispherical photographs taken with a self-leveling fish-eye camera 1m above the stream surface according to *Valverde and Silvertown* [1997]. The processing of these data is described in detail in *Groom et. al.* [2011a]. The upstream control reaches were established to provide a measure of year-to-year and spatial variability in temperature that occur independent of harvest. The treatment reaches were established to quantify stream temperature changes due to harvest. The downstream reaches were established to examine potential downstream temperature responses to any temperature changes occurring within the harvest unit. This paper focuses on modeling the dependence of change in maximum downstream temperature on change in maximum harvest reach temperature.

3. Analysis Methods

3.1. Linear Regression

In order to maintain continuity with previous previous RipStream studies we used the maximum daily temperature averaged over a 40-day mid-summer period from July 15 to August 23 as our temperature metric. We calculated this metric for the temperature probe locations 1W, 2W, 3W, 4W, denoted T_{1W}, T_{2W}, T_{3W}, T_{4W}, respectively. A temporal change in temperature across harvest, calculated as pre-harvest temperature subtracted from post-harvest temperature a each probe location i, is denoted by ΔT_i.

Figure 2 shows the experimental values of ΔT_{4W} for all sites in the study and we see a wide range of downstream responses. We hypothesized that the primary driver of ΔT_{4W} is the temperature change in the harvest reach, ΔT_{3W}, but that differences in downstream reach properties significantly contribute to the variation in downstream temperature response. In order to provide contrast to the NLC model and motivate its use, we examine the performance of a simple linear regression in describing the correlation between ΔT_{4W} and ΔT_{3W}. Figure 3 shows ΔT_{4W} plotted against ΔT_{3W} along with the linear regression. While the linear regression does describe the general trend in the data, it does not capture the variability in the data or provide insight into the underlying sources of this variation. The linear regression produced an R^2-value of 0.61 and is described by the function:

$$\Delta T_{4W}(C^\circ) = (0.5)\Delta T_{3W} - 0.041(C^\circ) \tag{1}$$

Note that site 7353, indicated in Figure 3, was not used in determining the best fit because its behavior was severely atypical as discussed in detail in section 4. The slope of the best fit line indicates that for forested streams of the type selected for this this study, the pre to post-harvest *change* in maximum temperature at a location approximately 300m downstream of harvest will be *on average*, 50% of that *change* at the harvest location. This result does not imply that the absolute water temperature must either decrease (cool) or increase (heat) as it moves downstream. The implications of this result and the NLC analysis are detailed in sections 5 and 6.

We see in Figure Figure 3 that the data deviate from the simple linear model, suggesting that ΔT_{3W} may not be the only source of the measured variation in ΔT_{4W} and that the behavior of any particular site can be quite different from the average behavior. The NLC model we have applied predicts this site-specific variation, indicating a significant deterministic contribution to the variation, as was hypothesized. The model also provides valuable information about the relative importance of measurable site-specific stream properties in determining the downstream response to temperature changes in the harvest reach.

3.2. Newton's Law of Cooling Model

Newton's Law of Cooling is an empirical relation which states that the rate of temperature change of an object is proportional to the difference between the object temperature and the equilibrium temperature, T_{eq} as described by equation 2.

$$\frac{dT}{dt} = \alpha(T_{eq} - T) \tag{2}$$

Here $\alpha = A_{eff}h_{eff}/C$, where C is the of heat capacity of the object, h_{eff} is the effective heat transfer coefficient describing the ease with which the object exchanges heat with the environment, and A_{eff} is the effective area across which heat exchange may occur. We begin by assuming that a parcel of stream water moving downstream will follow NLC and thus the rate of temperature change for the parcel is proportional to the difference between the parcel temperature and its environmentally determined equilibrium temperature. The equilibrium temperature of the parcel is defined as the temperature at which the net thermal energy flux into the parcel by all heat transfer mechanisms is zero. Consequently, the equilibrium temperature may be correlated with, but is not entirely represented by, the temperature of any particular environmental entity. Rather, the equilibrium temperature is a weighted average of the temperatures of all environmental entities with which the parcel exchanges energy, including, but not limited to, groundwater, the channel bed, the upper atmosphere, space, and the sun itself. Therefore, the equilibrium temperature is constantly changing on the diurnal as well as seasonal time scales.

For the specific case of a constant equilibrium temperature, the solution to equation 2 is:

$$T(t) = T_{eq} + [T_0 - T_{eq}]e^{-\alpha t} \tag{3}$$

The integrated form of Newton's Law of Cooling described by equation 3 is also often referred to as simply Newton's Law of Cooling, however we see that it also accounts for warming if $T_0 < T_{eq}$. Here T_0 is the object temperature at time $t = 0$ and T_{eq} is the constant equilibrium temperature.

The 40-day mid-summer average daily maximum temperature metric does not probe the diurnal cycle in stream temperature or T_{eq} and thus we approximate T_{eq} in the model as the yet-unknown 40-day average of T_{eq} at the time of day when stream temperature is a maximum at the probe location. Note that T_{eq} is not equal to the measured maximum stream temperature because the occurrence of maximum daily temperature measured at a specific stream location (our data) requires a rate of temperature change equal to zero in the Eulerian frame (at the probe location). This occurs when successive parcels arriving at the probe location each have the same temperature upon arrival. Conversely, the rate of temperature change in the Lagrangian frame is zero when the individual parcel to which the Lagrangian frame is attached reaches T_{eq}. We model the temperature of a parcel of water between temperature probes $3W$ and $4W$ in the Lagrangian frame using equation 3 with T_{eq} as an unknown. The heat capacity of the thermistor is negligible compared to that of the water parcel so the temperature measured at a specific probe location in the Eulerian frame is equal to the temperature of the water parcel passing over the probe at that time. Setting $t = 0$ when the parcel passes probe $3W$ at the end of the harvest reach and τ equal to the transit time between probes $3W$ and $4W$ allows conversion from the Lagrangian frame model temperature to the Eulerian frame measured temperature and we see that $T_{3W} = T(t = 0)$, $T_{4W} = T(t = \tau)$, and T_{eq} now represents the equilibrium temperature in the downstream reach, T_{4Weq}. Making these substitutions in equation 3 we arrive at:

$$T_{4W} = T_{4Weq} + [T_{3W} - T_{4Weq}]e^{-\alpha\tau} \tag{4}$$

This model assumes T_{eq} to be constant in space across the downstream reach and constant over the transit time, τ. This assumption requires that τ is small compared to the time over which T_{4Weq} and α change appreciably and that the length of the downstream reach is small compared to the distance over which T_{4Weq} and α change appreciably. Test-case velocity measurements suggest that τ for streams in this study are on the order of one hour, which may be pushing the boundaries of the previous assumptions. Consequently, this model and our subsequent analysis and conclusions are limited to the scale of a 300m reach. Applying equation 4 to the summers before and after harvest, subtracting the equation before from the equation after, and assuming that harvest does not affect T_{4Weq} or α or τ in the unharvested downstream reach, we modeled the change in downstream temperature, ΔT_{4W} as:

$$\Delta T_{4W} = \Delta T_{3W}e^{-\alpha\tau} + \Delta T_{4Weq}[1 - e^{-\alpha\tau}] \tag{5}$$

Here ΔT_{3W} and ΔT_{4Weq} are the changes in temperature of the $3W$ probe and the downstream reach equilibrium temperature, respectively. The data in Figure 3 support the linear dependence of ΔT_{4W} on ΔT_{3W} that is predicted by equation 5; however the data exhibit significant variation and deviation from the general linear fit applied to the 15 sites because the values of ΔT_{4Weq} and α and τ are site specific. We used measured values of gradient, wetted width, max depth, downstream reach length values, and changes in upstream control reach temperatures to approximate the site-specific values of these model variables.

3.3. Downstream Transit Time

The transit time of the downstream reach is modeled as $\tau = L/v$, where L is the downstream reach length and v is the flow speed in the downstream reach. In order to model the flow speed using gradient measurements we apply Manning's formula (*Subramanya* [2009]) which states that $v \propto G^{1/2}$, and we have:

$$\tau \propto \frac{L}{G^{1/2}} \tag{6}$$

Here G is the average gradient of the stream within the downstream reach, typically defined as length along the stream divided by change in elevation. The gradient of the streams in our study was measured at 60m intervals along the downstream reach. The G values we used in the model are an average of these gradient measurements for each site.

3.4. Heat Capacity of the Stream

The heat capacity of the modeled parcel of water is proportional to the volume of the parcel and consequently the cross sectional area of the stream, which is approximated by the wetted width, W of the stream multiplied by the maximum depth, D. The wetted width and maximum depth are measured at 60m intervals along the downstream reach and we use the average of these measurements W and D for each site.

$$C \propto WD \tag{7}$$

3.5. Downstream Shade Factor

Shade and shelter provided by stream side vegetation and local topography reduce solar heating during the day and radiative cooling at night and also reduce wind speed, and consequently convection and evaporation. We hypothesize that through these processes the level of downstream shade does influence the downstream response to temperature harvest and that models for h_{eff} and A_{eff} would incorporate the shade level. The downstream shade factor (fractional sky view), S of the study streams was determined from digital image analysis of hemispherical photographs taken 1m above the stream surface. However, the narrow range spanned by these measured downstream shade values does not provide enough information content for us to evaluate and validate a downstream shade component in the model, as discussed further in section 5.

3.6. Site-Specific Newton's Law of Cooling Model

Combining equations 6 and 7 we arrive at:

$$\alpha\tau = \phi \frac{L}{WDG^{1/2}} \tag{8}$$

Here ϕ is a model parameter incorporating the proportionality constants associated with equations 6 and 7. Given limited environmental and stream data, we are forced to assume that ϕ is approximately non-site specific for the streams in this study. This assumption is supported by the success of the model in predicting the downstream responses of the study streams and this generality is considered a positive feature of the model.

3.7. Downstream Equilibrium Temperature

Finally, we account for non-harvest related (e.g. climatic) fluctuations in stream temperature. We use stream temperature data taken at probes $1W$ and $2W$, which lie upstream from harvest to model these fluctuations. In the context of our NLC model, year-to-year changes in the local climate will influence actual stream temperature by changing T_{eq}. From equation 3 we see that $dT/dT_{eq} = 1 - e^{-\alpha t}$, which is constant for a given α and $t = \tau$ corresponding to a specific site. This result suggests that changes to T_{eq} cause proportional changes to stream temperature, so we approximate ΔT_{1Weq} and ΔT_{2Weq} as proportional to the change in control reach equilibrium temperature. Assuming that local changes in climate will affect the control reach and downstream reach equilibrium temperatures differently, but proportionally, ΔT_{4Weq} is modeled as:

$$\Delta T_{4Weq} = \beta \Delta T_{1W,2W} \tag{9}$$

Here $\Delta T_{1W,2W}$ is the average of ΔT_{1W} and ΔT_{2W}.

Inserting equations 8 and 9 into equation 5 we model the expected ΔT_{4W} using the measured upstream temperature changes, downstream reach length, and average values for gradient, wetted width and max depth using the equation:

$$\Delta T_{4W} = \Delta T_{3W} e^{-\phi \frac{L}{WDG^{1/2}}} + \beta \Delta T_{1W,2W} (1 - e^{-\phi \frac{L}{WDG^{1/2}}}) \tag{10}$$

In the following section we apply the model described by equation 10 to data from the study sites in order to understand the underlying causes of the downstream temperature responses exhibited by individual streams as well as the variability among those responses.

4. Modeling Results

We determined the model parameter values $\phi = 2 \times 10^{-4}(m)$ and $\beta = 1$ by a two parameter R^2 fit of the model to measured ΔT_{4W} data. The resulting R^2 value was 0.95. Figure 3 shows the measured and predicted values of ΔT_{4W} plotted against ΔT_{3W}. We see that the two-parameter NLC model does significantly better than the linear regression ($R^2 = 0.61$) at predicting the measured ΔT_{4W} values, despite having the same number of free parameters (two). We see in Panel A of Figure 4 that the difference between modeled and measured ΔT_{4W} values are all less than $0.4C^\circ$ in magnitude, with the exception of site 7353. At this site ΔT_{1W}, ΔT_{2W}, and ΔT_{3W} were all negative and yet ΔT_{4W} was positive. We therefore conclude that the increase in downstream temperature was not caused by harvest, but rather by some as yet-unknown local effect occurring in the downstream reach. The model uses temperature data taken upstream of the harvest reach to account for the effects of non-harvest related temperature fluctuations and thus can not account for the behavior of this site due to the localized nature of the downstream disturbance. Considering this result, site 7353 was not used in the fit to determine ϕ and β, a model predicted value of ΔT_{4W} for this site is not shown in Figure 3, and model data for this site are not shown in subsequent figures.

With the values of ϕ and β determined, we examine the relative contribution of each term in equation 10, where the first term approximates the contribution to downstream temperature change caused by the harvest reach temperature change, ΔT_{3W}, and the second term approximates the contribution by climatic changes to the downstream equilibrium temperature, ΔT_{4Weq}. Note that the measured ΔT_{3W} is caused by a combination of harvest and climate driven fluctuations in ΔT_{3Weq} so that the contributions of each term in equation 10 are not treated separately as purely harvest-induced and purely climate-induced contributions. Panel B of Figure 4 shows the value of ΔT_{4Weq} extracted from the model and panel C shows the relative contribution of the two terms in the model.

We also remove the effect of the site specific probe locations from the exponent in the NLC model and calculate $(\alpha\tau)/L = \phi/[WDG^{1/2}]$, which characterizes the site specific rate at which a water parcel will change temperature with distance traveled in the downstream reach. Relatively large values of $(\alpha\tau)/L$ indicate that the magnitude of the temperature change measured at a specific downstream location will decrease in a relatively short distance downstream while small values of $(\alpha\tau)/L$ indicate a relatively long distance required for substantial decrease in measured temperature change. Panel D of Figure 4 shows the site specific values of $(\alpha\tau)/L$. The range of behaviors produced by the variation in $(\alpha\tau)/L$ are illustrated in Figure 5, which shows the calculated profiles of the downstream temperature change $\Delta T_{4W}(x)$, that produced the measured $\Delta T_{4W}(x = L)$ data in response to ΔT_{3W} for a sample of the study streams. Note that these profiles do not represent the behavior of the absolute stream temperature, but rather behavior of the change in stream temperature across the harvest year.

5. Modeling Discussion

The NLC model allows for intuitive analysis of stream sites which might appear to have outlying behavior. For example, site 7854 (indicated in Figure 3) experienced a $-0.2C^{\circ}$ change in downstream temperature even though the harvest reach temperature experienced a relatively large measured temperature increase of $2.6C^{\circ}$. The model was able to predict that this site would behave well outside of the general trend defined by other sites. Examination of the stream variables in the context of the NLC model reveals that site 7854 experienced an overall decrease in the local equilibrium temperature, as seen in Panel B of Figure 4 and indicated by negative upstream control reach temperature changes across harvest ($\Delta T_{1W,2W} = -0.2C^{\circ}$). Site 7854 also possessed the second smallest WD value among all sites. This combination resulted in a relatively high rate of reduction in the temperature change, as seen in Figure 5. The NLC model shows us that the outlying behavior of this site was caused by this high rate of change coupled with a relatively long transit time for this site, due to a long downstream reach length of $L = 305m$ and third smallest gradient of $G = .023$. Note that removing site 7854 from the dataset does not change the values of ϕ and β produced by fitting the model to the data and only changes the R^2-value from 0.95 to 0.96. This result indicates that the NLC model would have predicted the unique behavior of this site even if it were not a part of the initial data set used to calibrate the model which highlights the predictive power of the model.

The ability of the model to reproduce the measured downstream responses using non-site-specific values for model parameters ϕ and β indicates that these values are relatively constant across the streams selected for this study. This result further suggests that once these parameters values are determined by comparison of model to data for a given type of stream in a given geographic region, the model might be used to predict the future downstream response to harvest of similar streams in that region. The value of $\beta = 1$ suggests that the downstream and control reach equilibrium temperatures respond to changes in climatic conditions by equal amounts, within the resolution of this model.

In order to leverage the predictive power of the NLC model, the site-specific L in equation 10 is replaced with a general distance variable, x. We set $\Delta T_{4Weq} = 0$ because we cannot know *a priori* the naturally occurring fluctuations to T_{4Weq}, thus we want an expression for the distance dependence of a change in downstream temperature caused purely by a harvest reach temperature change:

$$\Delta T_{4W}(x) = \Delta T_{3W} e^{-\phi \frac{x}{WDSG^{1/2}}} \tag{11}$$

We use equation 11 to calculate the ratio, $R(x)$, of ΔT_{4W} to ΔT_{3W} as function of distance downstream:

$$R(x) = \Delta T_{4W}(x)/\Delta T_{3W} = e^{-\phi \frac{x}{WDSG^{1/2}}} \tag{12}$$

Using average values for G and WD will allow us to estimate a characteristic behavior of the sites in our study. The solid line in Figure 6 shows $R(x)$ for the average values of $G = 0.047$ and $WD = 0.53m^2$. We see that for these average values the across-harvest-year change in downstream temperature drops to 60% of that change occuring in the harvest reach after 300m. These calculations are qualitatively supported by the site averaged, but less accurate, behavior predicted by the linear fit, which suggests a 50% reduction in temperature change after $\approx$ 300m. However, $R(x)$ is exponentially sensitive to G and WD and consequently these average behaviors cannot be assumed to describe any specifc site.

In order to produce bounding behaviors for the sites in the study we combined the extreme values of G and WD measured from all sites and used these in the model. The maximum measured values are $G = 0.10$ and $WD = 1.0m^2$ and the minimal values are $G = 0.02$, and $WD = 0.12m^2$. The bounding behaviors calculated from these two value sets are shown in Figure 6. We see that for the long-distance bounding case the downstream temperature change measured 300m from the end of the harvest reach would be 84% of the temperature change that occured at the end of the harvest reach ($R(x) = 0.84$). For the short-distance bounding case $R(x)$ is less than 1% after 300m. Values of $R(x = L) = e^{-\phi \frac{L}{WDSG^{1/2}}}$ calculated using the specific stream property values and reach lengths at each study site are also shown for comparison to the bounding behavior curves.

In order to examine the specific effects of ΔT_{4Weq} on downstream response we calculate $R(x)$ for theoretical example cases when $\Delta T_{4Weq} \neq 0$. In this case the form for $R(x)$ is more complex:

$$R(x) = \Delta T_{4W}(x)/\Delta T_{3W} = e^{-\phi \frac{x}{WDSG^{1/2}}} + [1 - e^{-\phi \frac{x}{WDSG^{1/2}}}] \frac{\Delta T_{4Weq}}{\Delta T_{3W}} \tag{13}$$

We see that calculating $R(x)$ for $\Delta T_{4Weq} \neq 0$ requires values for ΔT_{3W} and ΔT_{4Weq}. As seen in panel B of Figure 4, the range of values for ΔT_{4Weq} extracted from the model was approximately $-0.4C^\circ$ to $0.4C^\circ$. Figure 7 shows ΔT_{4W} calculated for ΔT_{4Weq} values of $-0.4C^\circ$ and $0.4C^\circ$ for the cases of the harvest reach temperature change being $1C^\circ$ and $3C^\circ$. We see that changes to ΔT_{4Weq} within this range do not significantly affect the rate at which ΔT_{4W} increases or decreases. However, integrated over distances of $300m$ this change in rate might affect the value of ΔT_{4W} by detectable levels ($\approx 0.3C^\circ$).

The wide range of behaviors spanned by the bounding behaviors exemplifies the exponential sensitivity of $R(x)$ to G and WD. These sensitivities are illustrated in Figures 8 and 9 which show $R(x = 150m)$ and $R(x = 300m)$ as a function of G and WD. The average of measured values of the variables not serving as the independent variable in the plots were used. We see that the slopes of these curves are significant within the range of values measured for these stream properties and thus the measured behavior is highly sensitive these properties. This analysis indicates that blanket statements about distance required for return to pre-harvest temperature and use of regional average or non-local variable values to model site-specific behavior may lead to miscalculations.

We find that within the range of *downstream* shade factor values measured in the study streams, S has no significant effect on the behavior of the model. Due to all measured values of S being near one, modeling the rate of temperature change α, as either proportional to, or inversely proportional to S does not significantly affect the fitted parameter values or the downstream behavior, whether the site-specific or average values were used. Figure 10 shows $R(x = 150m)$ and $R(x = 300m)$ for both model types, $\alpha \propto 1/S$ and $\alpha \propto S$. We see that within the range of S values measured, the slope of these curves is small relative to that in figures 8 and 9, which demonstrates relative insensitivity of the model to this variable within that range. The success of the model at describing the data despite the model insensitivity to S indicates that for streams with relatively uniform and undisturbed riparian conditions downstream of harvest, the values of G and WD will drive the variations in downstream temperature response.

6. Conclusions

We have developed a Newtons Law of Cooling model for prediction and analysis of stream temperature response to harvest activity. We used the NLC model to analyze the specific downstream responses to harvest study streams throughout the Oregon Coast Range by relating variables in the model to measured stream data. The necessary measured data were stream temperature change upstream from harvest, distance from harvest reach, gradient, wetted width, and max depth. We determined the two free model parameters, which were held constant across sites in the study, by comparing the output of the model to the experimental data. We found that the model allowed us to determine the sources of the significant variation in measured downstream temperature response to harvest and that the model provides an insightful tool for determining the dominant factors influencing downstream temperature response to harvest.

For the forested streams in our study the model suggests that on average harvest reach stream temperature changes exist at fractions near 50% 300m downstream, but that they do not persist indefinitely. The model also indicates that variation in stream morphology can lead to significant variability in downstream temperature response to harvest, and it allowed us to estimate limiting-case behaviors. We estimated that for streams similar to those in this study, the across-harvest-year temperature change 300m downstream of the harvest reach can range from 84% to less than 1% of the change in the harvest reach, in the absence of major naturally occuring stream temperature fluctuations.

This NLC model does not explicitly treat hyporheic flow or groundwater exchange; however, the effects of these processes on the rate of stream temperature change are included in the fitted model parameter ϕ. The fact that ϕ was held constant in this study suggests that these effects are roughly equally prevalent across the streams in the study. This study specifically selected streams without significant tributaries in the downstream reach and it is likely that the rate of reduction in downstream temperature change estimated here will be greater for streams with significant undisturbed tributaries.

Additional application of NLC modeling methods to stream temperature data should help to improve the NLC model accuracy and determine the range of stream, environmental, and treatment conditions under which the NLC model is valid and accurate. For example, data from a set of many temperature probes within downstream reaches would allow us to fit the NLC model to the spatial temperature data at each site and determine site-specific values for the model free parameters ϕ and β. Comparison of these site-specific parameter values to measured stream properties may allow us to indetify those properties with greatest influence on ϕ and β so that we might model these values directly and reduce the number of free parameters in the NLC model. Analysis of data from a set of streams with a wider range of downstream shade values might allow for the addition and validation of a downstream shade component in the model. Analysis of data from streams with a wider range of morphologies and environments would test the generality of the NLC model and provide a greater range of input variables against which to test, refine, and improve the NLC model.

Acknowledgments. This work was supported by the Oregon Department of Environmental Quality, the Oregon Department of Forestry, the Environmental Protection Agency, and Weyerhaueser NR. We thank the RipStream Technical Committee for helpful discussion. Data are available free of charge from the corresponding author, Jeremiah Groom, or from the Oregon Department of Forestrys Forest Practices Research and Monitoring Program (http://www.oregon.gov/ODF/Pages/index.aspx).

References

Bogan, T., O. Mohseni, and H. G. Stefan, (2003), Stream temperature-equilibrium temperature relationship, Water Resour. Res., **39** , 1245, doi:10.1029/2003WR002034.

Brazier, J.R. and G.W. Brown (1973), Buffer strips for stream temperature control, Forest Research Laboratory, School of Forestry, Oregon State University, Corvallis, Oregon.

Brown, G.W., (1969), Predicting temperatures of small streams, Water Resour. Res., **5**, 68-75, doi:10.1029/WR005i001p00068.

Brown, G.W., G.W. Swank, and J. Rothacher, Brown, G.W. (1970), Predicting the Effects of Clearcutting on Stream Temperature, **25**, J. Soil Water Conserv., 11-13., Water Temperature in the Steamboat Drainage, Pacific Northwest Forest and Range Expt. Sta., Forest Service, U.S. Dept of Agric., Portland. Oregon. Res. Paper PNW-1 19. 17 p.

Caissie, D. (2006), The thermal regime of rivers: a review, Freshwater Biol., **51**, 13891406, doi:10.1111/j.1365-2427.2006.01597.x.

Caissie, D., M.G. Satish and N. El-Jabi, (2005), Predicting river water temperatures using the equilibrium temperature concept with application on Miramichi River catchments (New Brunswick, Canada), Hydrol. Proc., **19**, 2137-2159, doi: 10.1002/hyp.5684.

Caldwell, J.E., K. Doughty, and K. Sullivan (1991), Evaluation of downstream temperature effects on type 4/5 waters, *Timber/Fish/Wildlife Report #TFW-WQ5-91-004*, Washington Dept. of Natural Resources, Olympia, WA. 71 p.

Cole, E. and M. Newton, (2013), Influence of streamside buffers on stream temperature response following clear-cut harvesting in western Oregon, Can. J. For. Res., **43**, 993-1005, doi:10.1139/cjfr-2013-0138.

Dent, L., D. Vick, K. Abraham, S. Schoenholtz, and S. Johnson, (2008), Summer temperature patterns in headwater streams of the Oregon Coast Range, J. Am. Water Resour. Assoc., **44**, 803-813, doi:10.1111/j.1752-1688.2008.00204.x.

Donato, M.M., (2002), A statistical model for estimating stream temperatures in the Salmon and Clearwater rivers in Idaho, U.S. Geological Survey, Water-Resources Investigations Report 02-4195, Boise, Idaho.

Edinger, J.E., D. W. Duttweiler, and J. C. Geyer, (1968), The response of water temperatures to meteorological conditions, Water Resour. Res., **4**, 1137-1143, doi:10.1029/WR004i005p01137.

Gomi, T., R. D. Moore and A. S. Dhakal, (2006), Headwater stream temperature response to clear-cut harvesting with different riparian treatments, coastal British Columbia, Canada, Water Resour. Res., **42**, W08437, doi:10.1029/2005WR004162.

Gravell, J.A. and T.E. Link, (2007), Influence of timber harvesting on headwater peak stream temperatures in a northern Idaho watershed, For. Sci., **53**,189-205.

Groom, J.D., L. Dent, L. Madsen, (2011a), Stream temperature change detection for state and private forests in the Oregon Coast Range, Water Resour. Res., **47**, W01501, doi:10.1029/2009WR009061.

Groom, J.D., L. Dent, L. Madsen, J. Fleuret, (2011b), Response of western Oregon (U.S.A.) stream temperatures to contemporary forest management, For. Ecol. Manage., **262**, 1618-1629, doi:10.1016/j.foreco.2011.07.012.

Janisch, J.E., S. M. Wondzell, and W. J. Ehinger, (2012), Headwater stream temperature: interpreting response after logging, with and without riparian buffers, Washington, USA, For. Ecol. Manage. **270**, 302-313, doi:10.1016/j.foreco.2011.12.035.

Johnson, S.L., (2003), Stream temperature: Scaling of observations and issues for modeling, Hydrol. Processes, **17**, 497-499, doi:10.1002/hyp.5091.

Johnson, S.L., (2004), Factors influencing stream temperatures in small streams: substrate effects and a shading experiment, Can. J. Fish. Aquat. Sci., **61**, 913-923, doi:10.1139/f04-040.

Kaufmann, P.R. and E.G. Robison, (1998), Environmental Monitoring and Assessment Program – Surface Waters: Field Operations and Methods for Measuring the Ecological Condition of Wadeable Streams, pp 77-118 *In:* EPA/620/R-94/004F. Office of Research and Devel., U.S. Envir. Protect. Agency, Washington, D.C.

Kibler, K.M., A.Skaugset, L.M. Ganio, and M. M. Huso, (2013), Effect of contemporary forest harvesting practices on headwater stream temperatures: Initial response of the Hinkle Creek catchment, Pacific Northwest, USA, For. Ecol. Manage., **310**, 680-691, doi:10.1016/j.foreco.2013.09.009.

Moore, R.D., D.L. Spittlehouse, and A. Story, (2005a), Riparian microclimate and stream temperature response to forest harvesting: a review, J. Am. Water Resour. Assoc., **41**, 813-834, doi:10.1111/j.1752-1688.2005.tb03772.x.

Rex, J.F., D. A. Maloney, P. N. Krauskopf, P. G. Beaudry, and L. J. Beaudry, (2012), Variable-retention riparian harvesting effects on riparian air and water temperature of sub-boreal headwater streams in British Columbia, For. Ecol. Manage., **269**, 259-270, doi:10.1016/j.foreco.2011.12.023.

Sinokrot, B.A. and H.G. Stefan, (1993), Stream temperature dynamics: measurements and modeling, Water Resour. Res., **29**, 2299-2312, doi:10.1029/93WR00540.

Story, A., R. D. Moore, and J. S. Macdonald, (2003), Stream temperatures in two shaded reaches below cutblocks and logging roads: downstream cooling linked to subsurface hydrology, Can. J. For. Res., **33**, 1383-1396, doi:10.1139/x03-087.

Subramanya, V., *Flow in Open Channels*,(McGraw-Hill, New Delhi, 110008).

Sugimoto, S., F. Nakamura, and A. Ito, (1997), Heat budget and statistical analysis of the relationship between stream temperature and riparian forest in the Toikanbetsu River basin, northern Japan, J. For. Res., **2**, 103-107, doi:10.1007/BF02348477.

Neumann, D.W., B. Rajagopalan, and E.A. Zagona, (2003), Regression model for daily maximum stream temperature, J. Environ. Eng., **129**, 667-674.

Valverde, T. and J. Silvertown, (1997), Canopy closure rate and forest structure, Ecology, **78**, 1555-1562, doi:10.2307/2266148.

Zwieniecki, M. and M. Newton, (1999), Influence of streamside cover and stream features on temperature trends in forested streams of western Oregon, West. J. Appl. For., **14** : 106-113.

[width=20pc]study

Figure 1. Diagram of field study design showing relative locations of control, harvest, and downstream reaches and control (1W, 2W), harvest (3W), and downstream (4W) water temperature probes.

[width=20pc]delta4W

Figure 2. Experimental ΔT_{4W} values for each site, calculated as the difference between T_{4W} measured before and after harvest.

[width=20pc]results2

Figure 3. Measured (blue dots) and NLC modeled (red circles) ΔT_{4W} plotted against ΔT_{3W}. The black line is a linear regression to the measured data. Parameter values used in the model were $\phi = 2 \times 10^{-4}(m)$ and $\beta = 1$. The goodness of fit between model and data is $R^2 = 0.95$. As discussed in Section 3.1 site 7353 was not used in determining the model parameter values and R^2 value.

[width=20pc]panel

Figure 4. Panel A: Error in predicting the measured ΔT_{4W}, calculated as measured value subtracted from NLC model values. Panel B: Site specific values of ΔT_{4Weq} calculated using the NLC model determined parameter value $\beta = 1$. Panel C: Site specific values of $\alpha\tau/L$ calculated using the NLC model determined parameter value $\phi = 2 \times 10^{-4}(m)$. Panel D: Relative contributions to the overall ΔT_{4W} by the change in harvest reach temperature (solid) and naturally occurring fluctuations to ΔT_{4Weq} (open) calculated using the NLC model and determined parameter values $\phi = 2 \times 10^{-4}(m)$, $\beta = 1$.

[width=20pc]distancemodel

Figure 5. Change in temperature doenstream of harvest reach, $\Delta T_{4W}(x)$, calculated as a function of distance from harvest reach for several example study sites using the NLC model (lines). Orange dots are measured change at zero distance downstream, $\Delta T_{4W}(x=0) = \Delta T_{3W}$, and colored dots are measured values of $\Delta T_{4W}(x=L)$ for each site. In all cases model parameter values were $\phi = 2 \times 10^{-4}(m)$ and $\beta = 1$ and site-specific values of WD, G, and $\Delta T_{1,2}$ were used.

[width=20pc]extreme

Figure 6. Calculated ratio of harvest reach and downstream temperature changes in the absence of natural stream fluctuations as a function of distance from harvest reach using maximum (red) minimum (blue) and average (green) measured values of G, and WD. Dots show this value calculated using values of G, and WD, and L for each site. In all cases $\Delta T_{4Weq} = 0C^{\circ}$ and model parameter values were $\phi = 2 \times 10^{-4}(m)$, $\beta = 1$.

[width=20pc]with4Weq

Figure 7. Distance dependence of ΔT_{4W} calculated for ΔT_{4Weq} values of $0C^{\circ}$ $-0.4C^{\circ}$ and $0.4C^{\circ}$ for the example cases of $\Delta T_{3W} = 1C^{\circ}$ and $\Delta T_{3W} = 3C^{\circ}$. The legend designates these values used to produce each curve as (ΔT_{3W}, ΔT_{4Weq}). Average measured values of G and WD were used and model parameter values were $\phi = 2 \times 10^{-4}(m)$, $\beta = 1$.

[width=20pc]gradient

Figure 8. Calculated ratio of downstream to harvest reach temperature changes at distances of 150m and 300m downstream from harvest reach as a function of downstream gradient in the absence of natural stream fluctuations. In all cases the average measured values for WD were used, $\Delta T_{4Weq} = 0C^{\circ}$, and model parameter values were $\phi = 2 \times 10^{-4}(m)$, $\beta = 1$.

[width=20pc]area

Figure 9. Calculated ratio of downstream to harvest reach temperature changes at distances of 150m and 300m downstream from harvest reach as a function of downstream cross sectional area in the absence of natural stream fluctuations. In all cases the average measured value for G was used, $\Delta T_{4Weq} = 0C^{\circ}$, and model parameter values were $\phi = 2 \times 10^{-4}(m)$, $\beta = 1$.

[width=20pc]shade

Figure 10. Calculated ratio of downstream to harvest reach temperature changes at distances of 150m and 300m downstream from harvest reach as a function of downstream shade in the absence of natural stream fluctuations. Average measured values of G and WD were used. In all cases $\Delta T_{4Weq} = 0C^{\circ}$ and model parameter values were $\phi = 2 \times 10^{-4}(m)$, $\beta = 1$.

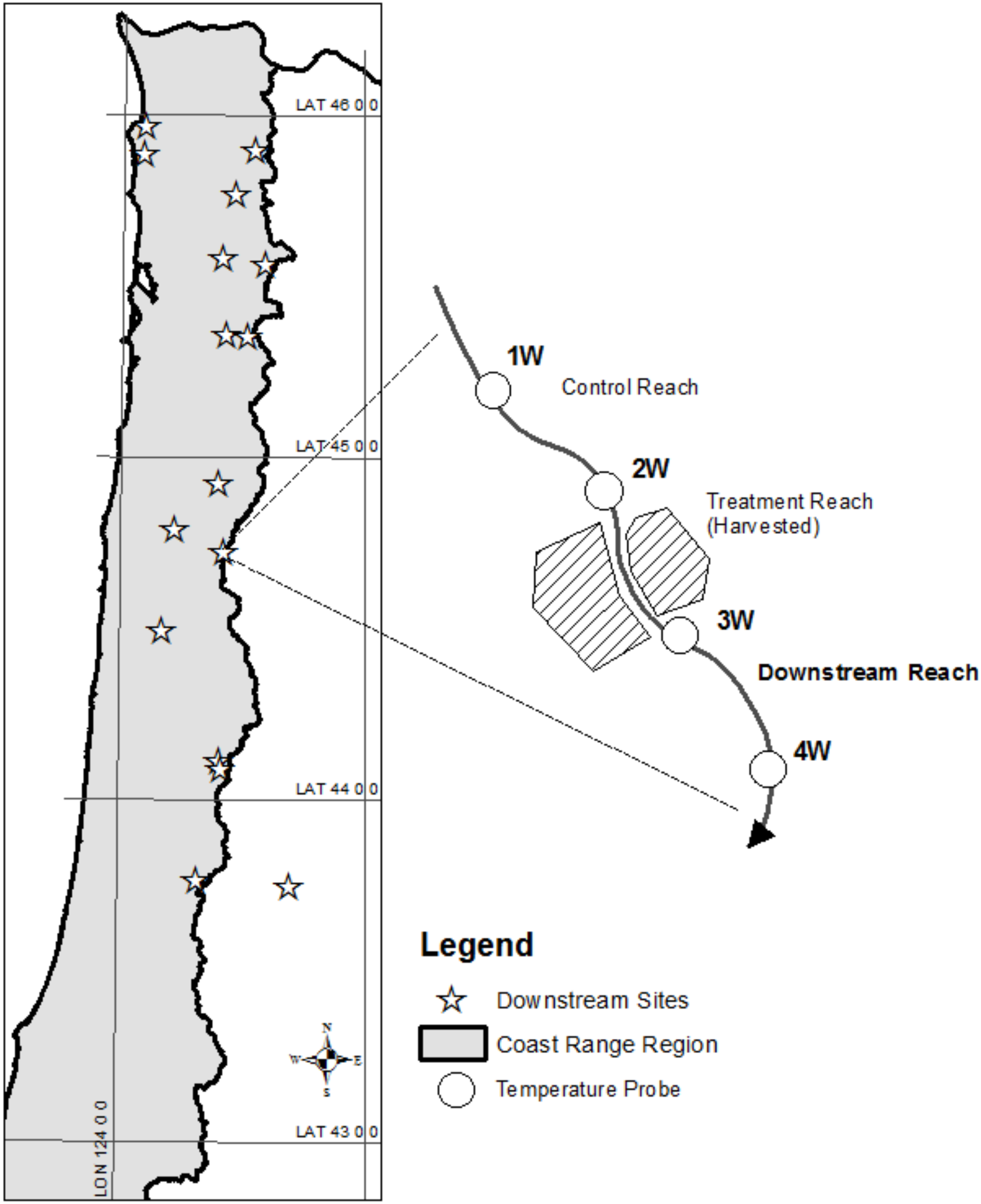

LAT 46 0 0
LAT 45 0 0
LAT 44 0 0
LAT 43 0 0
LON 124 0 0
1W
Control Reach
2W
Treatment Reach
(Harvested)
3W
Downstream Reach
4W
Legend
Downstream Sites
Coast Range Region
Temperature Probe
N
W
E
S

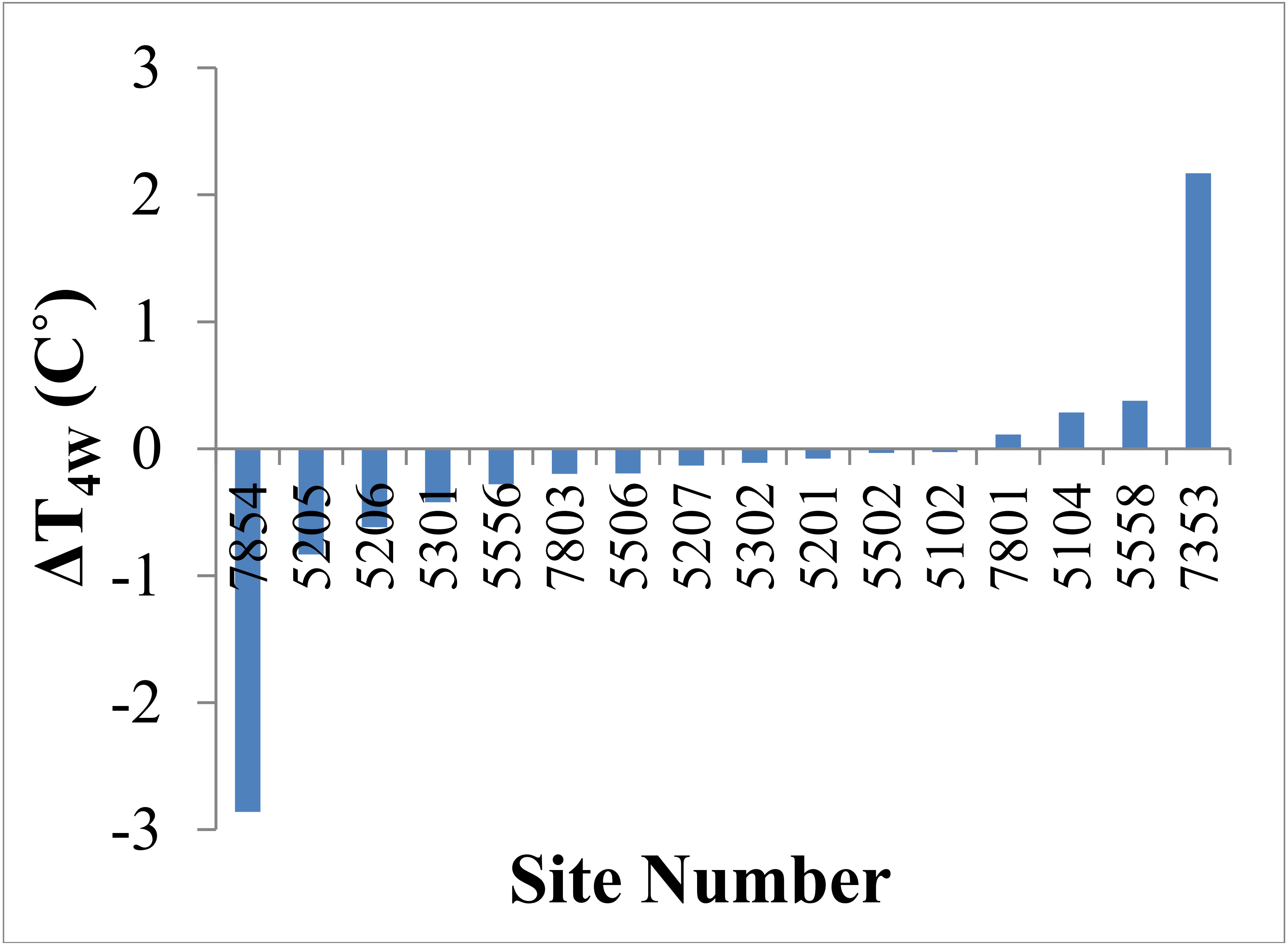
3
2
1
0
-1
-2
-3
ΔT4W (C°)
7854
5205
5206
5301
5556
7803
5506
5207
5302
5201
5502
5102
7801
5104
5558
7353
Site Number

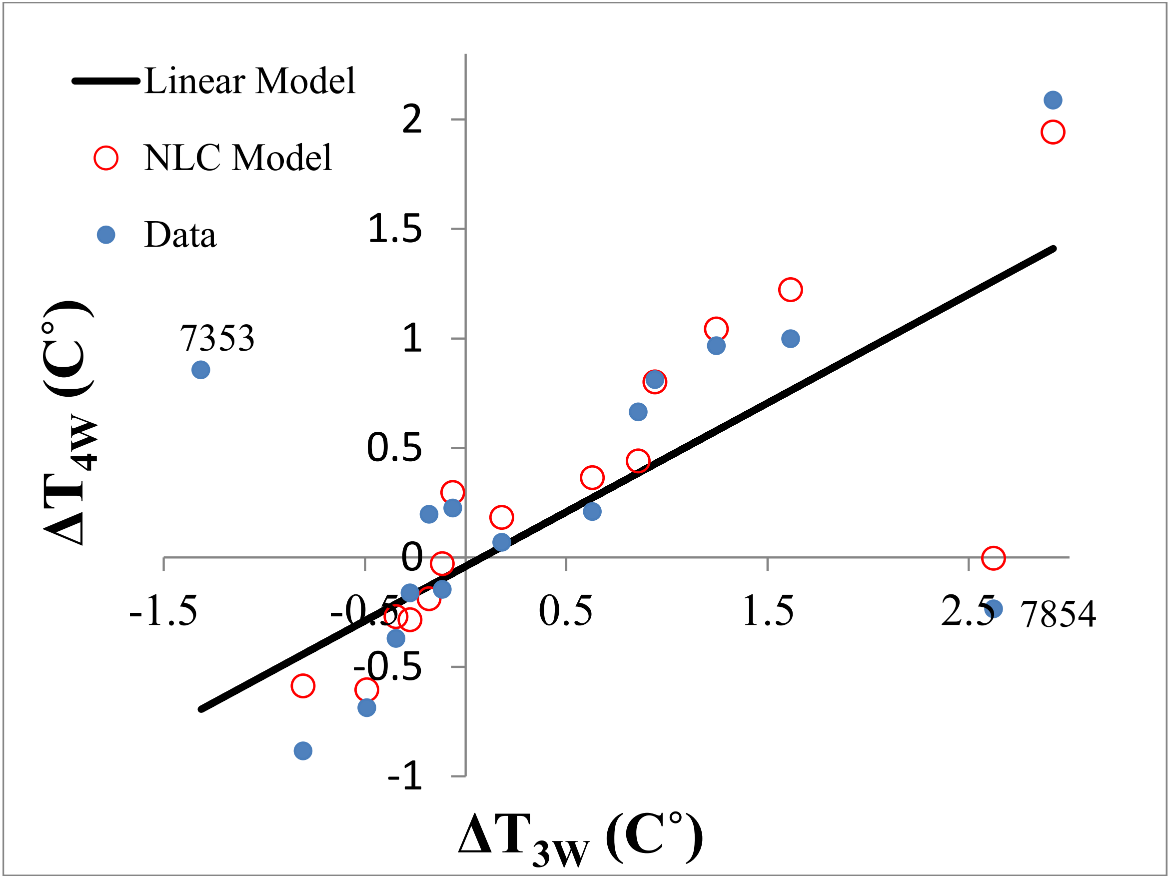
Linear Model
NLC Model
Data
7353
7854
2
1.5
1
0.5
0
-0.5
-1
-1.5
-0.5
0.5
1.5
2.5
ΔT_{4W} (C°)
ΔT_{3W} (C°)

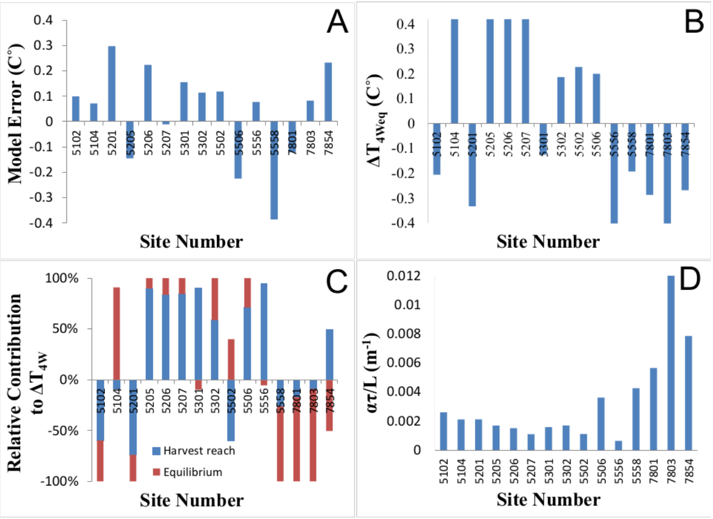
A
Model Error (C°)
0.4
0.3
0.2
0.1
0
-0.1
-0.2
-0.3
-0.4
5102 5104 5201 5205 5206 5207 5301 5302 5502 5506 5556 5558 7801 7803 7854
Site Number
B
ΔT4Weq (C°)
5102 5104 5201 5205 5206 5207 5301 5302 5502 5506 5556 5558 7801 7803 7854
Site Number
C
Relative Contribution to ΔT4W
100%
50%
0%
-50%
-100%
5102 5104 5201 5205 5206 5207 5301 5302 5502 5506 5556 5558 7801 7803 7854
Harvest reach
Equilibrium
Site Number
D
ατ/L (m-1)
0.012
0.01
0.008
0.006
0.004
0.002
0
5102 5104 5201 5205 5206 5207 5301 5302 5502 5506 5556 5558 7801 7803 7854
Site Number

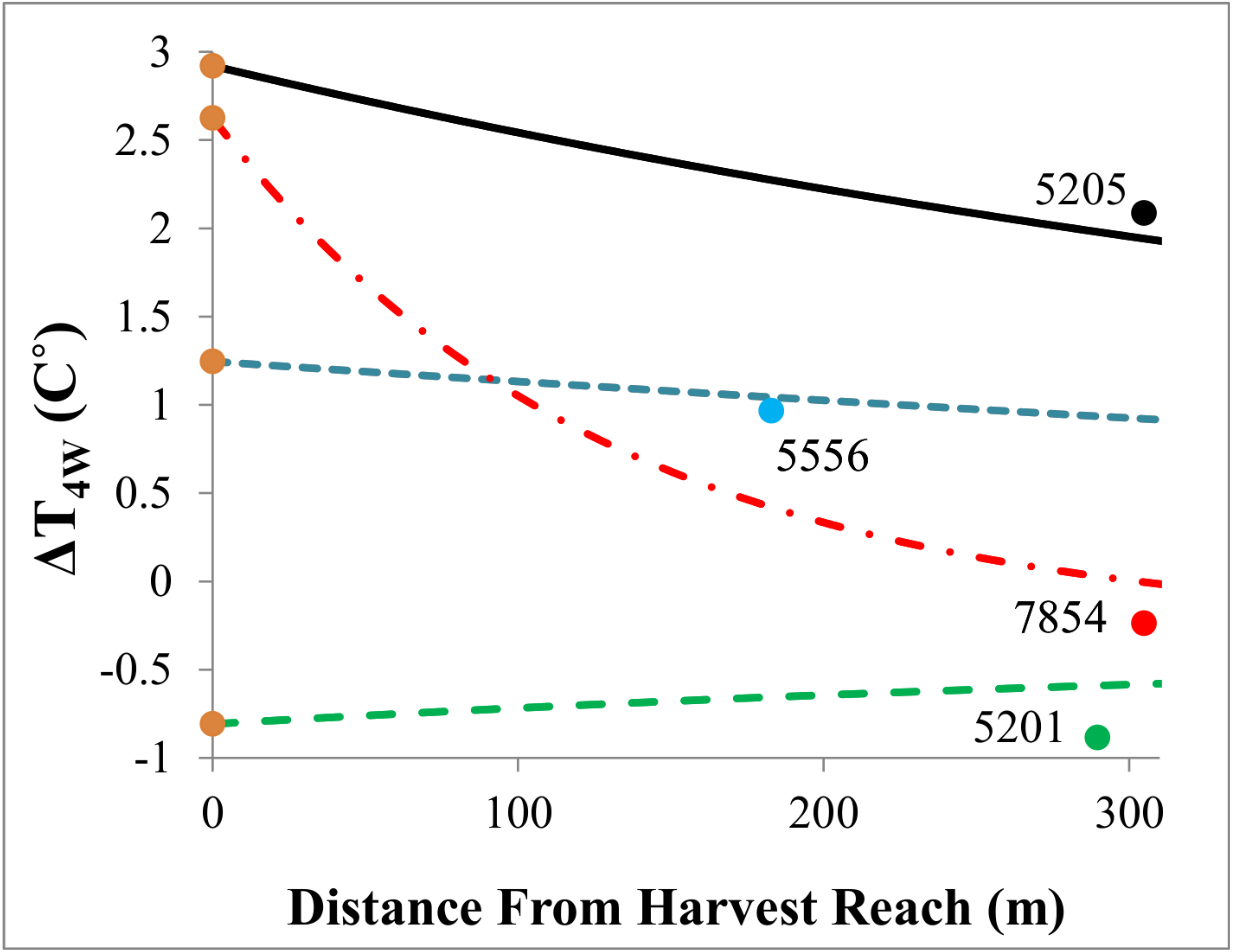
3
2.5
2
1.5
1
0.5
0
-0.5
-1
ΔT_{4W} (C°)
5205
5556
7854
5201
0
100
200
300
Distance From Harvest Reach (m)

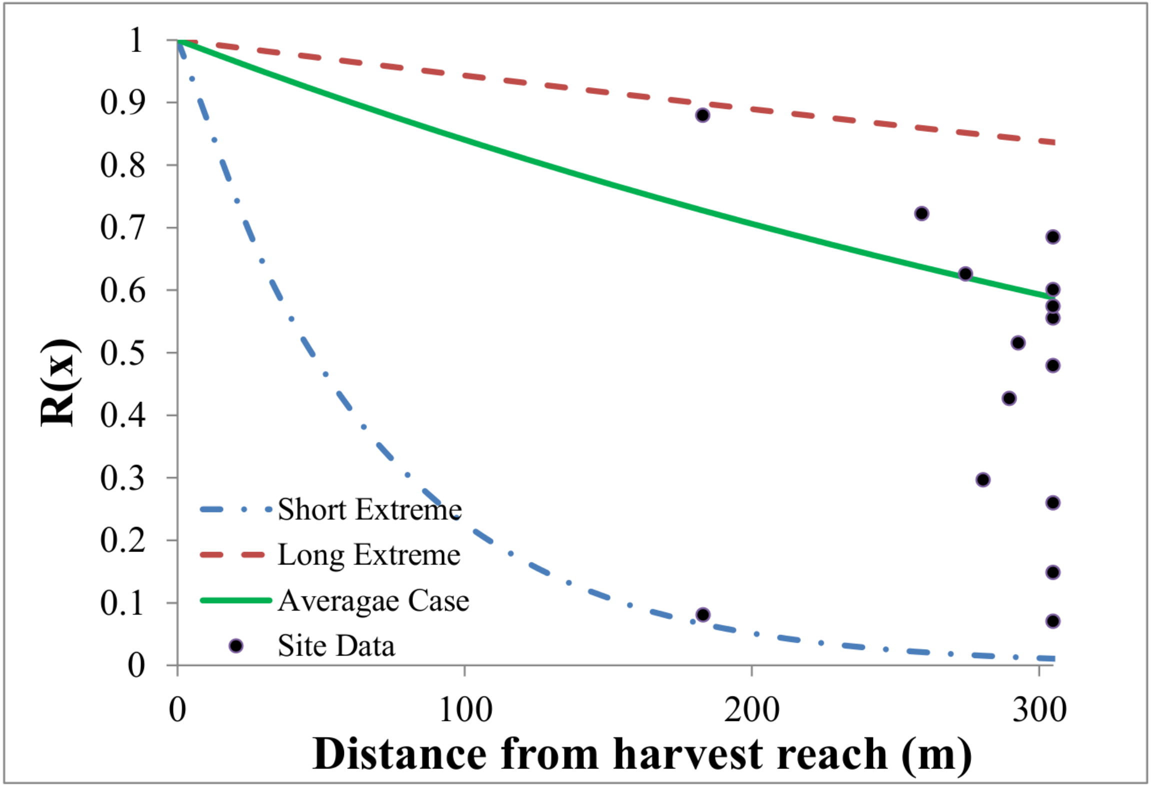
R(x)
1
0.9
0.8
0.7
0.6
0.5
0.4
0.3
0.2
0.1
0
0
100
200
300
Distance from harvest reach (m)
Short Extreme
Long Extreme
Averagae Case
Site Data

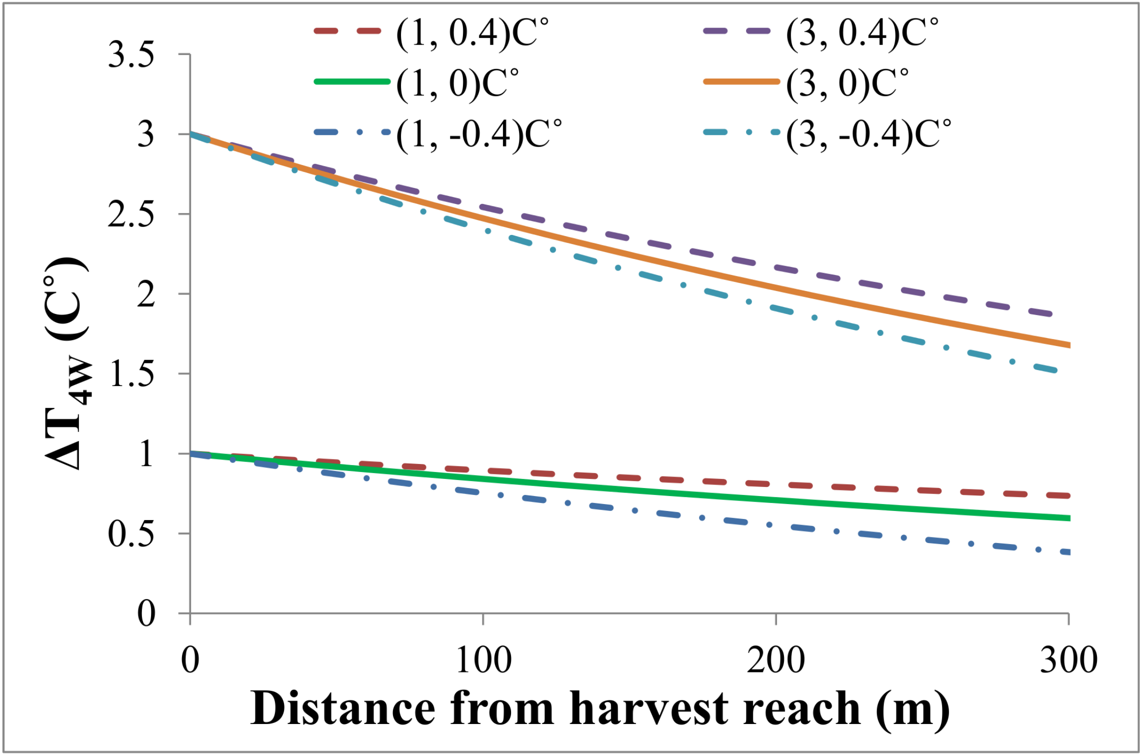

(1, 0.4)C°
(3, 0.4)C°
(1, 0)C°
(3, 0)C°
(1, -0.4)C°
(3, -0.4)C°
3.5
3
2.5
2
1.5
1
0.5
0
ΔT_{4w} (C°)
0
100
200
300
Distance from harvest reach (m)

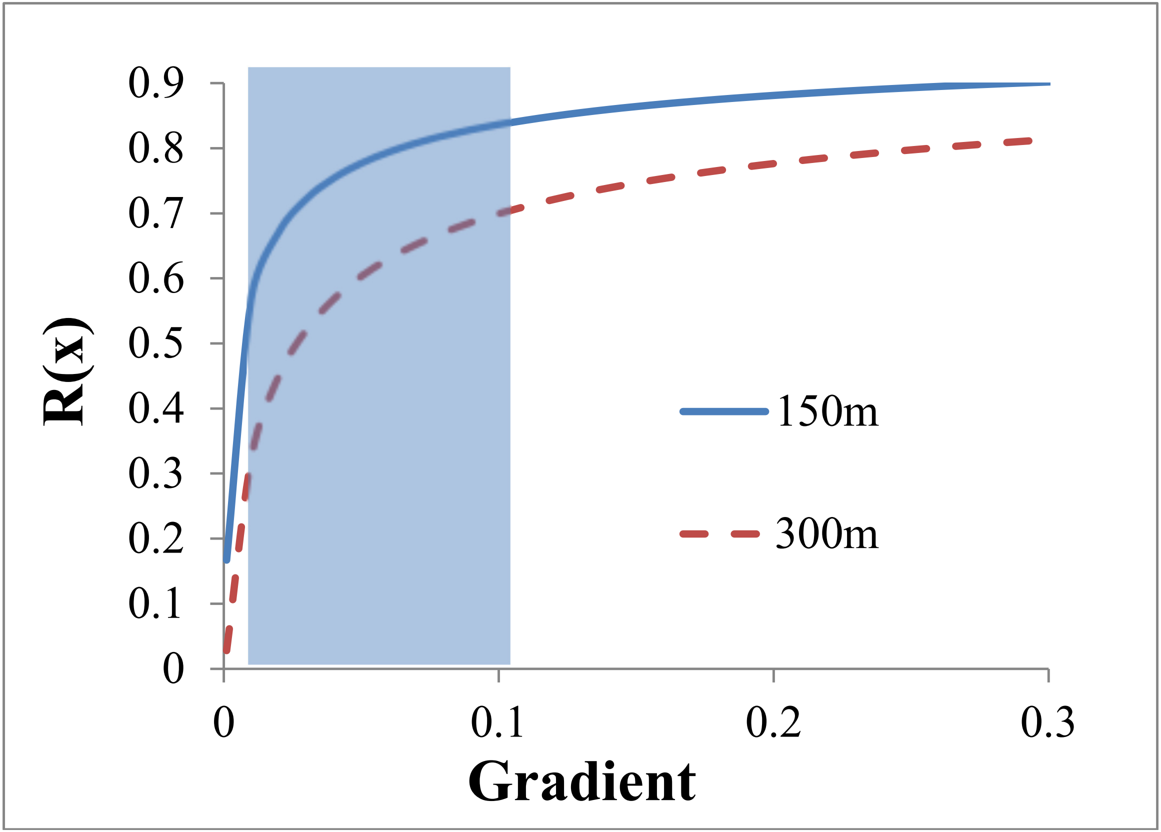

EPA-6822_000874

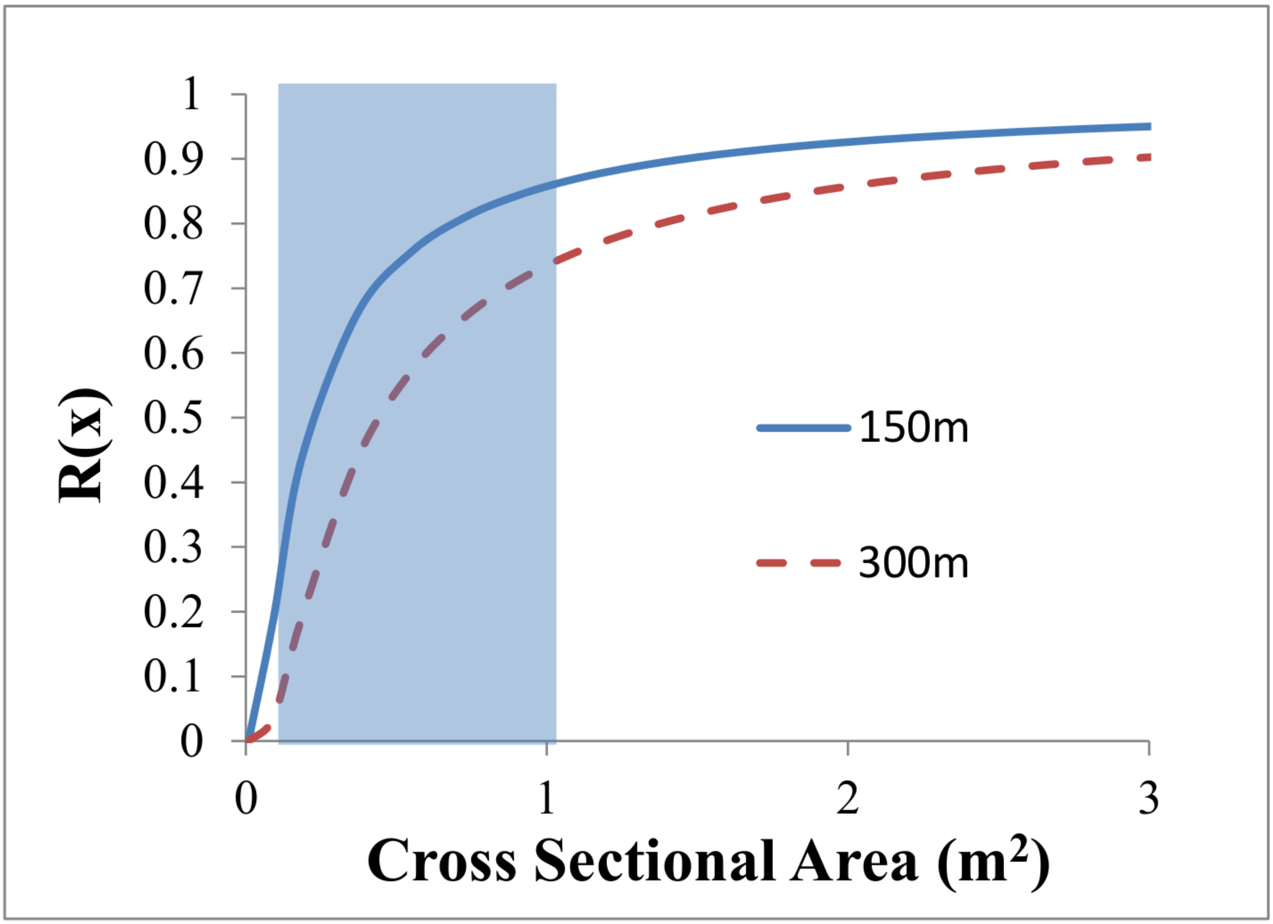

R(x)
1
0.9
0.8
0.7
0.6
0.5
0.4
0.3
0.2
0.1
0
0
1
2
3
Cross Sectional Area (m²)
150m
300m

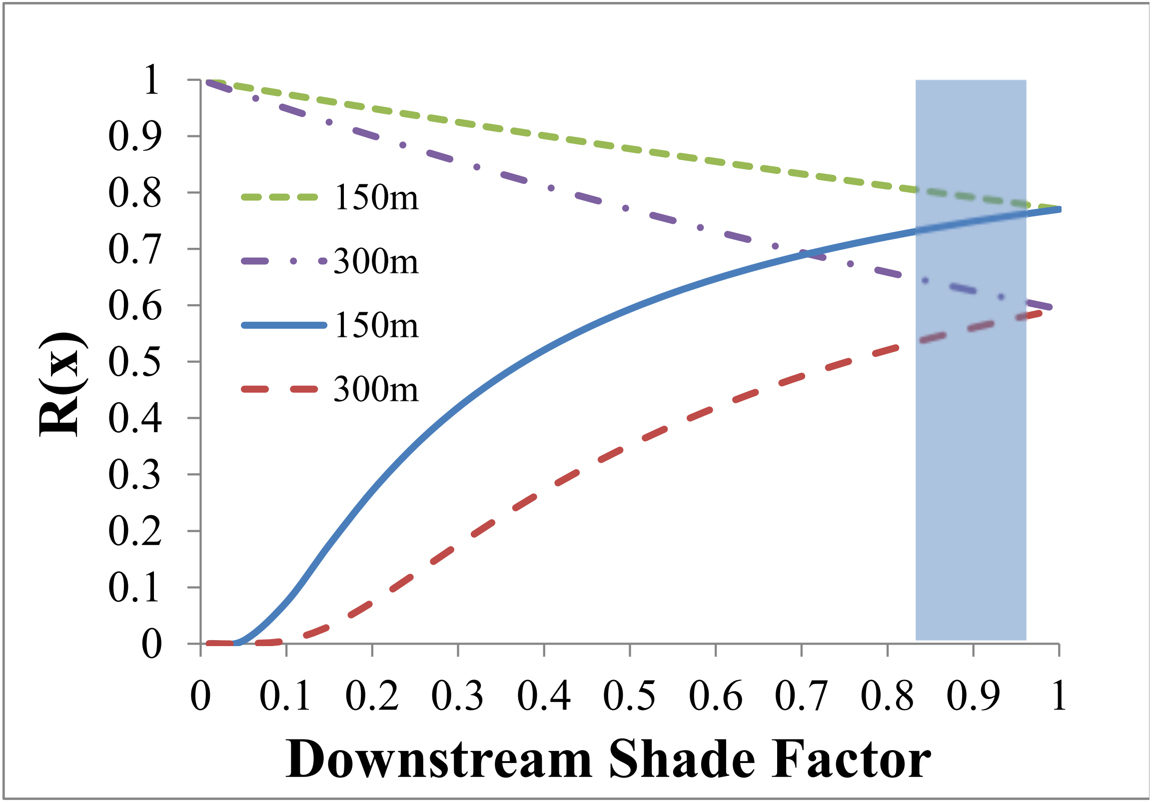

1
0.9
0.8
0.7
0.6
0.5
0.4
0.3
0.2
0.1
0
R(x)
150m
300m
150m
300m
0
0.1
0.2
0.3
0.4
0.5
0.6
0.7
0.8
0.9
1
Downstream Shade Factor